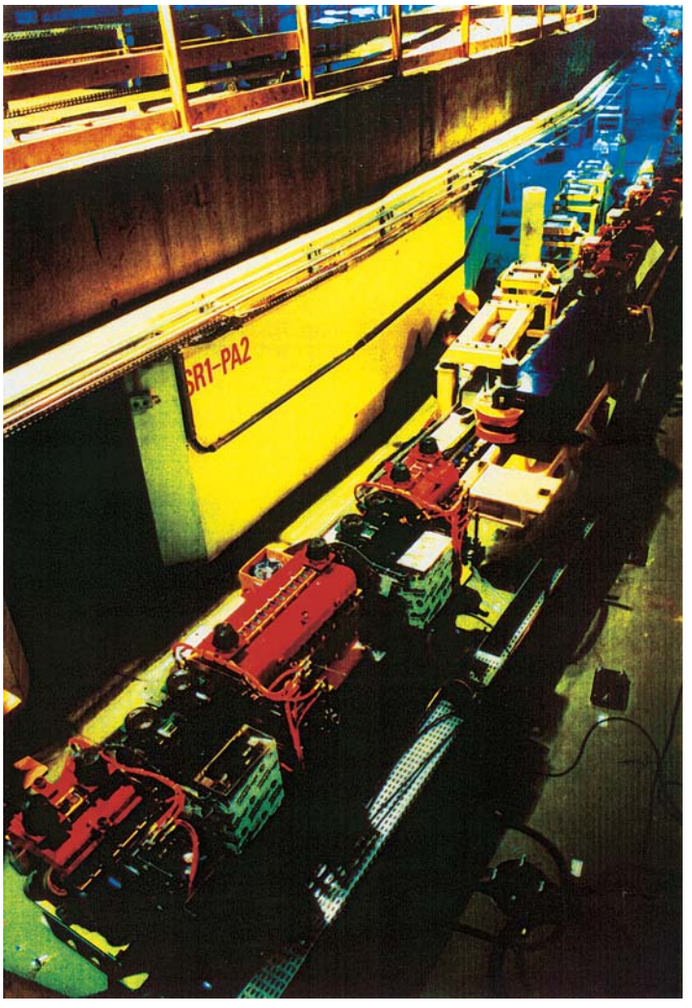

Fig. 8.1.2.3. The ring tunnel and part of the machine lattice at the ESRF, Grenoble, France.

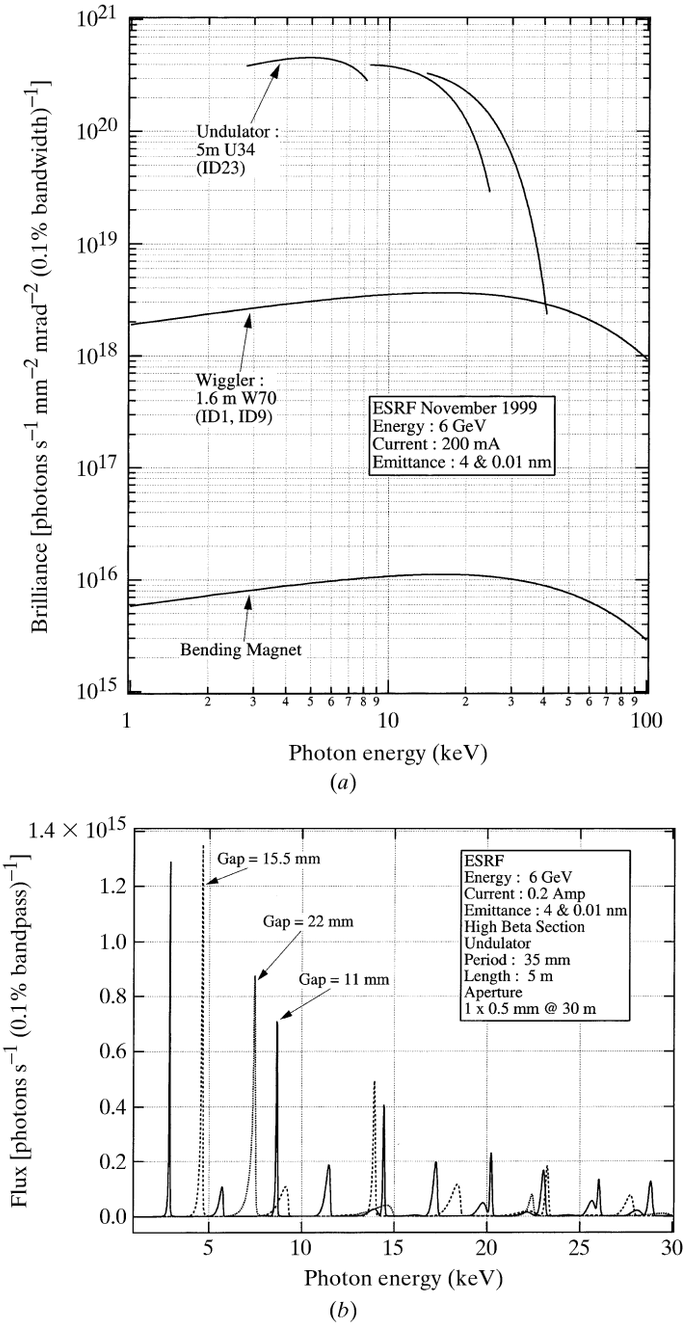

Fig. 8.1.2.4. SR spectra. (*a*) Brilliances of different SR source types (undulator, multipole wiggler and bending magnet) as exemplified by such sources at the ESRF. For the undulator, the tuning range (*i.e.* as the magnet gap is changed) is indicated. (*b*) Undulator-emitted spectra at the ESRF, shown as photon fluxes through a 1 × 0.5 mm aperture at 30 m, for three different gaps, *i.e.* widening the gap shifts the emitted fundamental and associated harmonics in each case to higher photon energies. Kindly provided by Dr Pascal Elleaume, ESRF, Grenoble, France.

sets a sample acceptance requirement to be met by the X-ray beam and machine emittance. A machine with an emittance that matches the acceptance of the sample greatly assists the simplicity and performance of the beamline optics (mirror and/or monochromator) design. The common beamline optics schemes are shown in Fig. 8.1.4.1.

In addition to the focal spot area and convergence angles, it is necessary to provide the appropriate spectral characteristics. In monochromatic applications, involving the rotating-crystal diffraction geometry, for example, a particular wavelength, λ, and narrow spectral bandwidth, $\delta\lambda/\lambda$, are used. Fig. 8.1.4.2(*a*) shows an example of a monochromatic oscillation diffraction photograph from a rhinovirus crystal as an example recorded at CHESS, Cornell. Fig. 8.1.4.2(*b*) shows the prediction of a white-beam broad-band Laue diffraction pattern from a protein crystal recorded at the SRS wiggler, Daresbury, colour-coded for multiplicity.

Table 8.1.4.1 lists the internet addresses of the SR facilities worldwide that currently have macromolecular beamlines.

8.1.5. Evolution of SR machines and experiments

8.1.5.1. *First-generation SR machines*

The so-called first generation of SR machines were those which were parasitic on high-energy physics operations, such as DESY in Hamburg, SPEAR in Stanford, NINA in Daresbury and VEPP in Novosibirsk. These machines had high fluxes into the X-ray range and enabled pioneering experiments. Parratt (1959) discussed the use of the CESR (Cornell Electron Storage Ring) for X-ray diffraction and spectroscopy in a very perceptive paper. Cauchois *et al.* (1963) conducted *L*-edge absorption spectroscopy at Frascati and were the first to diffract SR with a crystal (quartz). The opening experimental work in the area of biological diffraction was by Rosenbaum *et al.* (1971). In protein crystallography, multiple-

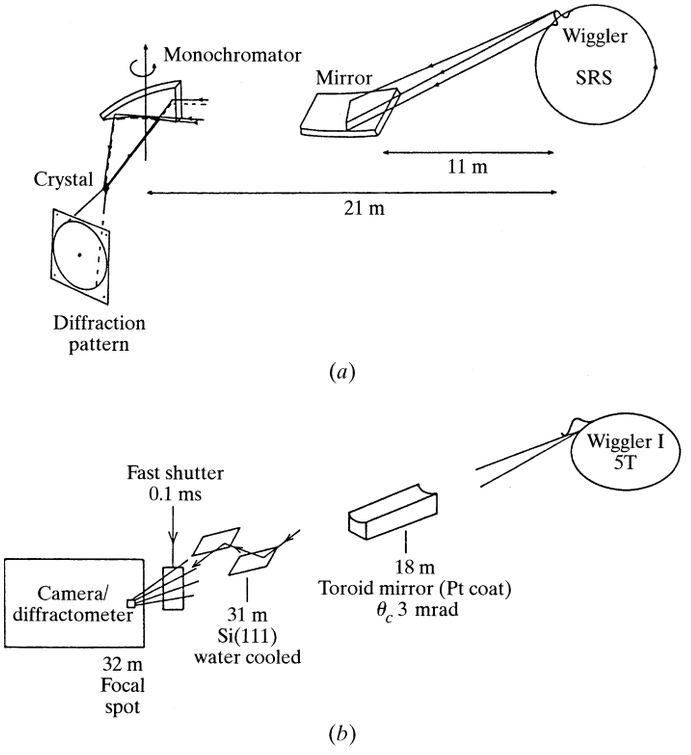

Fig. 8.1.4.1. Common beamline optics modes. (*a*) Horizontally focusing cylindrical monochromator and vertical focusing mirror [shown here for station 9.6 at the SRS (adapted from Helliwell *et al.*, 1986)]. (*b*) Rapidly tunable double-crystal monochromator and point-focusing toroid mirror [shown here for station 9.5 at the SRS (adapted from Brammer *et al.*, 1988)].

wavelength anomalous-dispersion effects (Fig. 8.1.5.1) were used from the onset (Phillips *et al.*, 1976, 1977; Phillips & Hodgson, 1980; Webb *et al.*, 1977; Harmsen *et al.*, 1976; Helliwell, 1977, 1979), and a reduction in radiation damage was seen (Wilson *et al.*, 1983) for high-resolution data collection. Historical insights into the performances of those machines, from the current-day perspective, are described in detail, for example, by Huxley & Holmes (1997) at DESY, Munro (1997) at Daresbury, and Doniach *et al.* (1997) at Stanford. A principal limitation was the problem of source movements, which degraded the focusing of the source onto a small crystal or single fibre and thus degraded the intrinsic brilliance of the beam; see, for example, Haslegrove *et al.* (1977), who advocated machine shifts dedicated to SR as a working compromise with the high-energy physicists. Some possible applications discussed were unfulfilled until brighter sources became available. The two-wavelength crystallography phasing method of Okaya & Pepinsky (1956) (see also Hoppe & Jakubowski, 1975) and the three-wavelength method of Herzenberg & Lau (1967), as well as the implementation of the algebraic method of Karle (1967, 1980, 1989, 1994), awaited more stable beams, which had to be rapidly and easily tunable over a fine bandpass ($<10^{-3}$). Experiments to define the anomalous-dispersion coefficients, including dichroism effects, at a large number of wavelengths at several example absorption edges in a variety of crystal structures were conducted at SPEAR (Phillips *et al.*, 1978; Templeton *et al.*, 1980, 1982; Templeton & Templeton, 1985). Values of f' over a continuum of wavelengths in a real compound (*i.e.*, not a metal in the gas phase) (Fig. 8.1.5.1*b*) were explored in a profile approach (now called DAFS, diffraction anomalous fine structure) by Arndt *et al.* (1982) at the newly commissioned SRS, the first dedicated second-generation SR source (see Section 8.1.5.2).

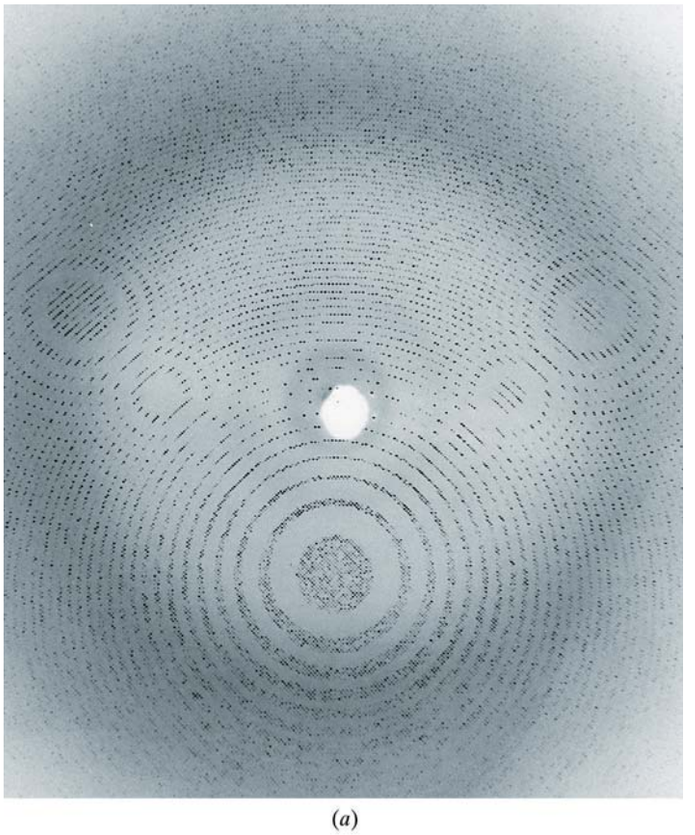

(*a*)

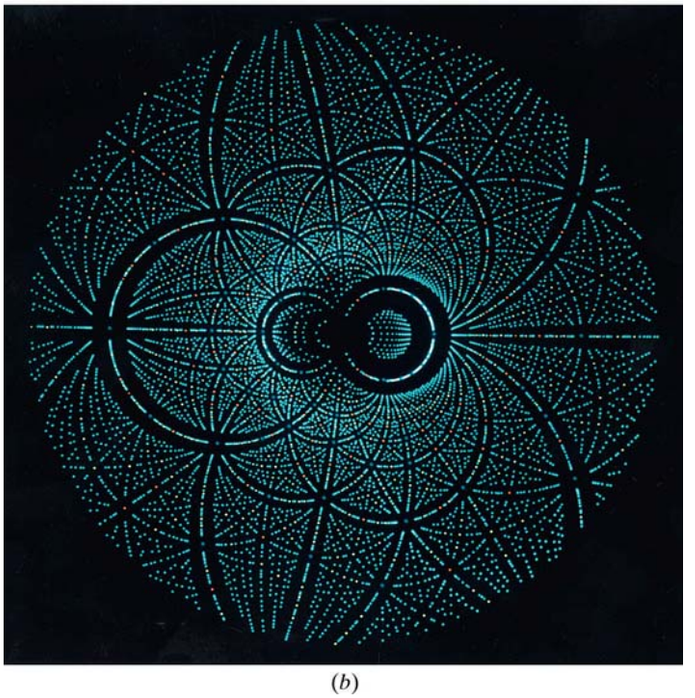

(*b*)

Fig. 8.1.4.2. Single-crystal SR diffraction patterns. (*a*) Rhinovirus monochromatic oscillation photograph recorded at CHESS (Arnold *et al.* 1987; see also Rossmann & Erickson, 1983). Copyright (1987) International Union of Crystallography. (*b*) Prediction of a protein crystal Laue diffraction pattern (for an illuminating bandpass, without monochromator, $\sim 0.4 < \lambda < 2.6$ Å). The colour coding is according to the multiplicity of each spot: turquoise for singlet reflections, yellow for doublets, orange for triplets and blue for quartet or higher-multiplicity Laue spots. Reproduced with permission from Cruickshank *et al.* (1991). Copyright (1991) International Union of Crystallography.

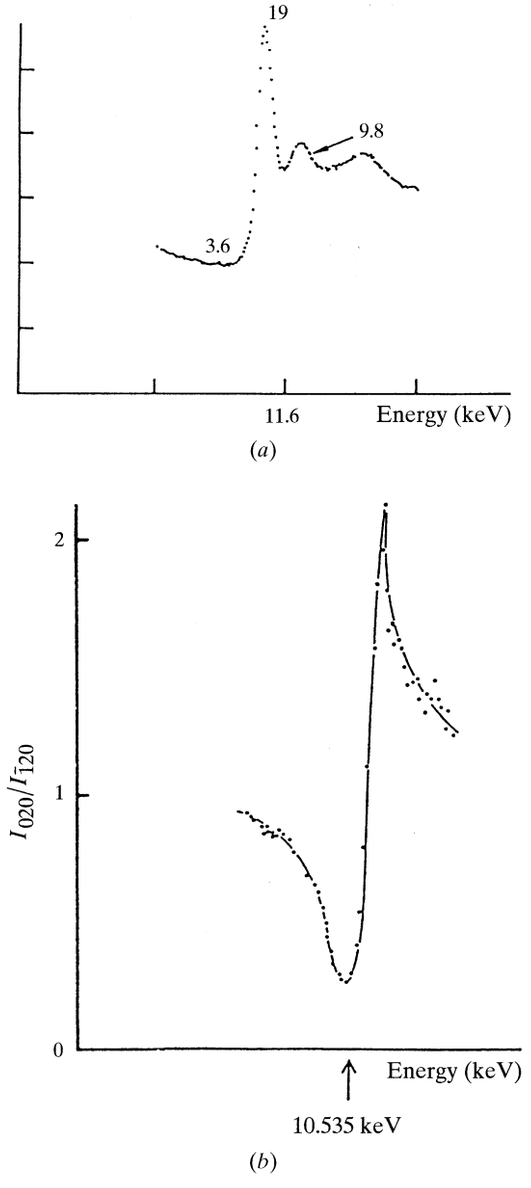

Fig. 8.1.5.1. Anomalous dispersion. (*a*) f'' as represented by an absorption spectrum [Pt L_{III} edge for $K_2Pt(CN)_4$ as the example] (Helliwell, 1984). Reproduced with the permission of the Institute of Physics. (*b*) f' as estimated by a continuous polychromatic profile method. Reproduced with permission from *Nature* (Arndt *et al.*, 1982). Copyright (1982) MacMillan Magazines Limited.

8.1.5.2. *Second-generation dedicated machines*

The building of dedicated X-ray sources began with the SRS at Daresbury, which came online in 1980, having followed the NINA synchrotron (closed in 1976) and the associated Synchrotron Radiation Facility at Daresbury. Elsewhere in the world, LURE (Lemonnier *et al.*, 1978) and CHESS at Cornell were building up their SR macromolecular crystallography operations in the late 1970s and early 1980s, and the NSLS in Brookhaven and the Photon Factory (PF) in Japan were both under construction. The NSLS and the PF came online in 1983 and 1984, respectively. Thus, there was a rapid increase in the number of operating machines and beamlines worldwide in the X-ray region for protein crystallography. There were teething problems with the SRS with the r.f. cavity window problem, interrupting operation for many months in 1983, and at the NSLS in its early period due to vacuum chamber problems.

Table 8.1.5.1. *A comparison of the parameter list for the 2 GeV SRS, 1997, and the new higher-energy machine for the UK, DIAMOND*

S/C = superconducting magnet; MW = multipole wiggler (permanent magnet design).

	SRS *	DIAMOND †
Storage ring energy	2 GeV	3 GeV ‡
Circumference	96 m	350 m §
Beam emittance	110 nm rad	15 nm rad
Beam current after injection	300 mA	300 mA
Typical dipole beam source sizes (σ)		
horizontal	900 μm	400 μm
vertical	200 μm	150 μm
Critical energy		
dipole	3.2 keV	20 keV (S/C)
wiggler	13.3 keV (S/C)	10 keV (MW)

* From Munro (1997).
† From Suller (1994) and Suller (1998).
‡ Up to 3.5 GeV.
§ A larger circumference is now proposed.

Pioneering experiments continued and blossomed. Seminal work ensued in virus crystallography [Rossmann & Erickson (1983) at Hamburg and Daresbury; Usha *et al.* (1984) at LURE], Laue diffraction for time-resolved protein crystallography [Moffat *et al.* (1984) at CHESS; Helliwell (1984, 1985) at the SRS; Cruickshank *et al.* (1987, 1991); Hajdu, Machin *et al.* (1987); Helliwell *et al.* (1989); Bourenkov *et al.* (1996); Neutze & Hajdu (1997)], enzyme catalysis in the crystal [Hajdu, Acharya *et al.* (1987) at the SRS], MAD [Phillips *et al.* (1977); Einspahr *et al.* (1985); Hendrickson (1985); Hendrickson *et al.* (1989) at SPEAR, the SRS and the PF; Guss *et al.* (1988) at SPEAR; Kahn *et al.* (1985) at LURE; Korszun (1987) at CHESS; Mukherjee *et al.* (1989) and Peterson *et al.* (1996) at the SRS; Hädener *et al.* (1999) at the SRS and the ESRF, to cite a few experiments], protein crystallography involving isomorphous replacement with optimized anomalous scattering [Baker *et al.* (1990) at the SRS; Dumas *et al.* (1995) at LURE], small crystals [Hedman *et al.* (1985) at the SRS] and diffuse scattering with SR [Doucet & Benoit (1987); Caspar *et al.* (1988); Glover *et al.* (1991)].

8.1.5.3. *Third-generation high-brilliance machines*

As early as 1979, there were discussions on planning a proposal for a high-brilliance, insertion-device-driven European synchrotron-radiation (ESR) source. A wide variety of discussion documents and workshops, and the ESR project led by B. Buras and based in Geneva at CERN, culminated in the so-called 'Red Book' in 1987, the *ESRF Foundation Phase Report* (1987), totalling some 1000 pages of machine, beamline and experimental specifications and costs. This, then, was the progenitor of the third-generation sources, characterized by their high energy and high brilliance, tailored to optimized undulator emission in the 1 Å range. Actually, the ESRF machine energy was initially set at 5 GeV, but increased to 6 GeV to optimize the production of 14.4 keV photons to better match the nuclear scattering experiments proposed initially by Mossbauer in 1975. Proposals for the US machine, the Advanced Photon Source at 7 GeV, and the Japanese 8 GeV SPring-8 machine followed, with the higher machine energy enhancing the X-ray tuning range of undulators. Thus, MAD

tuning-based techniques were facilitated with these machines and studies involving ultra-small samples (crystals, single fibres, or tiny liquid aliquots) or very large unit cells were enabled. As a result, micron-sized protein crystals as well as huge multi-macromolecular biological structures (of large viruses, for example) also became accessible.

8.1.5.4. *New national SR machines*

Today a variety of enhanced national SR machines are being proposed and/or built. In the UK there is the DIAMOND 3 GeV machine and in France there is SOLEIL. The SLS in Switzerland, the country's first SR light source, is under construction. These machines are more tailored to the bulk of a country's user needs, distinct from the special provisions at the ESRF. The different countries' SR needs, of course, have many aspects in common, with some historical biases. The new sources are, in essence, characterized by high brilliance, *i.e.*, low emittance. The 2 GeV high-brilliance SR source ELETTRA in Trieste, the MAXII machine in LUND and the Brazilian Light Source are already operational. In many ways, national sources like the SRS, LURE, DORIS and so on fuelled the case and specification for the ESRF. Now the developments at the ESRF, including high harmonic emission of undulators *via* magnet shimming (Elleaume, 1989) and narrow-gap undulator operation (Elleaume, 1998), are fuelling ideas and the specification of what is possible in these new national SR sources. Table 8.1.5.1 compares the parameters of the mature SRS of 1997 (from Munro, 1997) with the proposed design for DIAMOND (Suller, 1994). A shift of emphasis to high brilliance is again clear, as the applications of SR involving small samples dominate. Likewise, a 3 GeV machine energy is indicative of the need to include a provision of high photon energies for many applications, including, obviously, access to short-wavelength absorption edges. The extent to which undulators, for <3 GeV, will reach the hard X-ray region at high brilliance (*e.g.* around 1 Å wavelength) will depend on the minimum undulator magnet gaps realizable, along with magnet shimming to improve high harmonic emission. Moreover, longer wavelengths in protein crystallography are being explored on lower-energy SR machines (*e.g.* <3 GeV) at >1.5 Å, even 2.5 Å (Helliwell 1993, 1997*a*; Polikarpov *et al.*, 1997; Teplyakov *et al.*, 1998), and even softer wavelengths are under active development to utilize the S *K* edge for anomalous dispersion (Stuhrmann & Lehmann, 1994). Such developments interact closely with machine and beamline specifications. At very short ($\sim$0.5 Å) and ultra-short ($\sim$0.3 Å) wavelengths, a high machine energy yields copious flux output; pilot studies have been conducted in protein crystallography at CHESS (Helliwell *et al.*, 1993) and at the ESRF (Schiltz *et al.*, 1997).

8.1.5.5. *X-ray free electron laser (XFEL)*

In terms of the evolution of X-ray sources, mention should be made of the X-ray free electron laser (XFEL); it now seems feasible that this will yield wavelength output well below the visible region of the electromagnetic spectrum. At DESY in Hamburg (Brinkmann *et al.*, 1997) and at SLAC (Winick, 1995), such considerations and developments are being pursued. Compared to SR, one would obtain a transversely fully coherent beam, a larger average brilliance and, in particular, pulse lengths of $\sim$200 fs full width at half-maximum with eight to ten orders of magnitude larger peak brilliance. Such a machine is based on a linear accelerator (linac)-driven XFEL utilizing a linear collider installation (*e.g.*, for a high-energy physics centre-of-mass energy capability of 500 GeV). For this machine there is a 'switchyard' distributing the electrons in a beam to different undulators from which the X-rays are generated in the range 0.1 to $\sim$12 keV. The anticipated r.m.s. opening angle would be 1 mrad and the source diameter would be 20 µm. This source of X-rays would then compete in time resolution with laser-pulse-generated X-ray beams [see Helliwell & Rentzepis (1997) for a survey of that work and a comparison with synchrotron radiation] and would also have higher brilliance.

8.1.6. SR instrumentation

The divergent continuum of X-rays from the source must be intercepted by the sample cross-sectional area. The crystal sample acceptance, as seen above, is a good way to illustrate to the machine designer the sort of machine emittances required. Likewise, the beamline optics, mirrors and monochromators should not degrade the X-ray beam quality. Mirror surface and shape finish have improved a great deal in the last 20 years; slope errors of mirrors, even for difficult shapes like polished cylinders, which on bending give a toroidal reflecting surface, are now around 1 arc second (5.5 µrad) for a length of 1 m. Thus, over focusing distances of 10–20 m, say, the focal-spot smearing contribution from this is 55–110 µm, important for focusing onto small crystals. Choice of materials has evolved, too, from the relatively easy-to-work with and finish fused quartz to silicon; silicon having the advantageous property that at liquid-nitrogen temperature the expansion coefficient is zero (Bilderback, 1986). This has been of particular advantage in the cooling of silicon monochromators at the ESRF, where the heat loading on optics is very high. An alternative approach with the rather small X-ray beams from undulators is the use of transparent monochromator crystals made of diamond, which is a robust material with the additional advantage of transparency, thus allowing multiplexing of stations, one downstream from the other, fed by one straight section of one or more undulator designs. For a review of the ESRF beamline optics, see Freund (1996); for reviews of the macromolecular crystallography programmes at the ESRF, see Miller (1994), Branden (1994) and Lindley (1999), as well as the *ESRF Foundation Phase Report* (1987). See also Helliwell (1992), Chapter 5.

Detectors have been, and to a considerable extent are still, a major challenge. The early days of SR use saw considerable reliance on photographic film, as well as single-counter four-circle diffractometers. Evolution of area detectors, in particular, has been considerable and impressive, and in a variety of technologies. Gas detectors, *i.e.*, the multiwire proportional chamber (MWPC), were invented and developed through various generations and types [Charpak (1970); for reviews of their use at SR sources, see *e.g.* Lewis (1994) and Fourme (1997)]. MWPCs have the best detector quantum efficiency (DQE) of the area detectors, but there are limitations on count rate (local and global) and their use at wavelengths greater than $\sim$1 Å is restricted. The most popular devices and technologies for X-ray diffraction pattern data acquisition today are image plates (IPs), mainly, but not exclusively, with online scanners [Miyahara *et al.* (1986); for a recent review, see Amemiya (1997)], and charge coupled devices (CCDs) (Tate *et al.* 1995; Allinson, 1994; Westbrook & Naday, 1997). Image plates and CCDs are complementary in performance, especially with respect to size and duty cycle; image plates are larger, *i.e.*, with many resolution elements possible, but are slower to read out than CCDs. Both are capable of imaging well at wavelengths shorter than 1 Å and with high count rates. Both have overcome the tedium of chemical development of film! Impressive performances for macromolecular crystallography are described for image plates (in a Weissenberg geometry) by Sakabe (1983, 1991) and Sakabe *et al.* (1995), and for CCDs by Gruner & Ealick (1995). Other detectors needed for crystallography include those for monitoring the beam intensity; these must not interfere with the beam collimation, and yet must monitor the beam downstream of the collimator (Bartunik *et al.*, 1981); also needed are fluorescence

references